Intestinal epithelial cell endoplasmic reticulum stress promotes MULT1 up-regulation and NKG2D-mediated inflammation

Intestinal epithelial cell endoplasmic reticulum stress promotes MULT1 up-regulation and NKG2D-mediated inflammation

Shuhei Hosomi,[1,3]* Joep Grootjans,[1,4]* Markus Tschurtschenthaler,[5] Niklas Krupka,[1] Juan D. Matute,[1,2] Magdalena B. Flak,[1] Eduardo Martinez-Naves,[6] Manuel Gomez del Moral,[7] Jonathan N. Glickman,[8] Mizuki Ohira,[3] Lewis L. Lanier,[9,10] Arthur Kaser,[4]** and Richard Blumberg[1]**

[1]Department of Medicine, Division of Gastroenterology, Brigham and Women's Hospital and [2]Division of Newborn Medicine, Boston Children's Hospital, Harvard Medical School, Boston, MA
[3]Department of Gastroenterology, Osaka City University Graduate School of Medicine, Osaka, Japan
[4]Department of Gastroenterology and Hepatology, Academic Medical Center, University of Amsterdam, Amsterdam, Netherlands
[5]Department of Medicine, Division of Gastroenterology, University of Cambridge, Cambridge, England, UK
[6]Department of Microbiology and Immunology and [7]Department of Cell Biology, Facultad de Medicina, Universidad Complutense de Madrid, Madrid, Spain
[8]Gastrointestinal Pathology Division, Miraca Life Sciences, Newton, MA
[9]Department of Microbiology and Immunology and [10]Parker Institute for Cancer Immunotherapy, University of California, San Francisco, San Francisco, CA

Endoplasmic reticulum (ER) stress is commonly observed in intestinal epithelial cells (IECs) and can, if excessive, cause spontaneous intestinal inflammation as shown by mice with IEC-specific deletion of X-box–binding protein 1 (*Xbp1*), an unfolded protein response–related transcription factor. In this study, *Xbp1* deletion in the epithelium ($Xbp1^{\Delta IEC}$) is shown to cause increased expression of natural killer group 2 member D (NKG2D) ligand (NKG2DL) mouse UL16-binding protein (ULBP)–like transcript 1 and its human orthologue cytomegalovirus ULBP via ER stress–related transcription factor C/EBP homology protein. Increased NKG2DL expression on mouse IECs is associated with increased numbers of intraepithelial NKG2D-expressing group 1 innate lymphoid cells (ILCs; NK cells or ILC1). Blockade of NKG2D suppresses cytolysis against ER-stressed epithelial cells in vitro and spontaneous enteritis in vivo. Pharmacological depletion of $NK1.1^+$ cells also significantly improved enteritis, whereas enteritis was not ameliorated in *Recombinase activating gene* $1^{-/-}$;$Xbp1^{\Delta IEC}$ mice. These experiments reveal innate immune sensing of ER stress in IECs as an important mechanism of intestinal inflammation.

INTRODUCTION

A defining feature of intestinal surfaces, which are subject to many types of inflammatory and neoplastic diseases (Smith et al., 2013), is the presence of a single layer of polarized epithelial cells that differentiate into distinct subtypes that function as a front-line defense of the mucosal barrier in the gut (Baker et al., 2014; Peterson and Artis, 2014). As a consequence of this anatomical location and its proximity to substantial quantities of environmental challenges, as well as the high demand for significant levels of secretory function to manage these needs, the intestinal epithelial cell (IEC) is highly dependent on the unfolded protein response (UPR) and autophagy to attenuate the significant levels of ER stress that occur to maintain homeostasis (Jia et al., 2011; Kaser et al., 2011; Bartolome et al., 2012; Grootjans et al., 2016). Indeed, ER stress and active autophagy are demonstrable under homeostatic conditions in humans and in mouse models and further increase in inflammatory bowel disease, especially in the small intestine (Bogaert et al., 2011; Deuring et al., 2014). Recent evidence shows that the UPR and/or autophagy are particularly important for mucin-secreting goblet cells and Paneth cells, which are located at the base of small intestinal crypts and secrete multiple antimicrobial peptides, as well as factors that sustain the intestinal stem cell niche (Ouellette, 2010; Salzman et al., 2010). As such, in situations of improperly folded epithelial-specific proteins (Heazlewood et al., 2008) or a disabled IEC-associated UPR (Kaser et al., 2008; Deuring et al., 2014), susceptibility to colitis or spontaneous enteritis that emanates directly from the epithelium emerges (Kaser et al., 2008; Todd et al., 2008; Adolph et al., 2013). However, the mechanisms by which ER stress of the IEC is

*S. Hosomi and J. Grootjans contributed equally to this paper.

**A. Kaser and R. Blumberg contributed equally to this paper.

Correspondence to Richard Blumberg: rblumberg@partners.org; Arthur Kaser: ak729@cam.ac.uk

Abbreviations used: ATF4, activating transcription factor 4; BALL, B acute lymphoblastic leukemia; ChIP, chromatin immunoprecipitation; CHOP, C/EBP homology protein; E:T, effector/target; EOMES, eomesodermin; H&E, hematoxylin and eosin; IEC, intestinal epithelial cell; IEL, intraepithelial lymphocyte; iIEL, intestinal IEL; ILC, innate lymphoid cell; IRE1α, inositol requiring enzyme 1α; MIC, MHC class I chain-related; MULT1, mouse ULBP-like transcript 1; qPCR, quantitative PCR; Tg, thapsigargin; ULBP, UL16-binding protein; UPR, unfolded protein response; Xbp1, X-box–binding protein 1.

The Rockefeller University Press
J. Exp. Med. 2017 Vol. 214 No. 10 2985–2997
https://doi.org/10.1084/jem.20162041

recognized by intestinal immune cells and how this then is converted into intestinal inflammation is unclear.

Driven by the abundance of data on early immune recognition of diseased epithelial cells in the setting of cancer (Raulet and Guerra, 2009), we set out to investigate surface expression of MHC class I and MHC class I–like proteins on ER-stressed IECs. Although we did not find differences in MHC class I surface expression, we demonstrate that ER stress in IECs up-regulates NK group 2 member D ligands (NKG2DL), specifically cytomegalovirus UL16-binding proteins (ULBPs) in the human or the orthologous mouse ULBP-like transcript 1 (MULT1; encoded by *Ulbp1*) proteins in mouse IECs in a pathway that involves C/EBP homology protein (CHOP; encoded by *Ddit3*), a major component of the UPR, within the IECs. We further show that up-regulation of NKG2DL contributes to the development of inflammation, as pharmacological blockade of the receptor for NKG2DL, NKG2D, reduces NKG2D-mediated killing in vitro and dampens inflammation in vivo. Finally, we show that NKG2D-expressing intraepithelial group 1 innate lymphoid cells (ILCs; NK cells or ILC1) in particular, but not NKG2D-expressing γδ T cells, play an important role in the inflammatory response to ER stress, as group 1 ILCs accumulate in response to stress in the epithelium, and their inhibition through blockade of NKG2D ameliorates ER stress–induced inflammation.

RESULTS

Epithelial ER stress induces surface expression of MULT1

To address whether ER stress can induce expression of NKG2D ligands on the surface of epithelial cells, we investigated the mouse small IEC line MODE-K, which was transfected with a short hairpin X-box–binding protein 1 (Xbp1 [*shXbp1*]) lentiviral vector (Kaser et al., 2008). Efficiency of short hairpin knockdown was confirmed by quantitative PCR (qPCR; Fig. S1 A). Interestingly, *shXbp1* MODE-K cells expressed higher levels of NKG2DL MULT1 and, to a lesser extent, retinoic acid early inducible 1 (RAE-1) on their cell surface compared with control MODE-K cells (shCtrl) but not H60 (Fig. 1, A and B). In contrast, expression of MHC class I, which is recognized by NK cell inhibitory receptors, was not affected by *Xbp1* knockdown in vitro and knockout in vivo, as shown with previously described $Xbp1^{\Delta IEC}$ mice that possess conditional deletion of *Xbp1* in the intestinal epithelium using the *Villin* (V) promotor to drive *Cre* expression (Fig. S1, C and D; Kaser et al., 2008). Furthermore, we treated shCtrl and *shXbp1* MODE-K cells with the ER calcium pump inhibitor thapsigargin (Tg) to investigate the effects of acute and generalized ER stress, as opposed to specific deletion of *Xbp1*. Interestingly, treatment with Tg induced *Ulbp1* (Mult1), but not *Raet1*, mRNA expression in both shCtrl and *shXbp1* MODE-K cells (Fig. 1, C and D). Increased *Ulbp1* mRNA expression was followed by induction of MULT1 protein surface expression (Fig. 1 E). As posttranscriptional regulation of NKG2DL by microRNA binding to the 3′ untranslated regions has been reported as one of the important mechanisms of NKG2DL expression (Stern-Ginossar et al., 2008; Himmelreich et al., 2011), we examined *Ulbp1* mRNA stability. Importantly, *Xbp1* silencing in MODE-K cells did not affect the stability of *Ulbp1* mRNA in the presence of actinomycin D treatment (Fig. S1 B), indicating that transcriptional induction is the mechanism of MULT1 expression on ER-stressed IECs.

We investigated whether NKG2DL up-regulation in MODE-K cells was specific for ER stress or whether it could also be elicited via other stimuli, such as through TLR ligands. Indeed, none of the TLR ligands increased MULT1 or RAE-1 surface expression on epithelial cells (Fig. 1, F and G). Together, these in vitro experiments demonstrated that ER stress in IECs preferentially targets the NKG2DL MULT1. Therefore, we focused our attention on MULT1 and investigated whether induction of MULT1 in response to ER stress also occurs in vivo. Indeed, *Ulbp1* expression was increased in small intestinal epithelial scrapings of mice with conditional deletion of *Xbp1* in IECs (Fig. 1 H) via nuclear translocation of a Cre-ER^{T2} recombinase fusion protein after its activation with tamoxifen ($V\text{-}CreER^{T2}\text{;}Xbp1^{fl/fl}$; hereafter called $Xbp1^{T\text{-}\Delta IEC}$). Further proof for the up-regulation of *Ulbp1* in response to epithelial ER stress in vivo was obtained by in situ hybridization of wild-type mice ($V\text{-}Cre^{-/-}\text{;}Xbp1^{fl/fl}$) and $Xbp1^{\Delta IEC}$ mice ($V\text{-}Cre^{+/-}\text{;}Xbp1^{fl/fl}$), as increased mRNA transcripts were clearly visualized in IECs of $Xbp1^{\Delta IEC}$ mice (Fig. 1 I). Lastly, we confirmed that NKG2DLs were also up-regulated in the human IEC line HT29. In line with the data obtained in mice, Tg-induced ER stress in HT29 cells selectively induced ULBP-1, -5 and -6, the human counterparts of MULT1, on both the mRNA (Fig. 2 A) and protein levels (Fig. 2 B), indicating that ER stress–induced up-regulation of NKG2DLs is conserved across mammalian species. In support of this, *ULBPs* were also induced in other human epithelial cell lines exposed to ER stress, including gastric (AGS), esophageal (EC-Gl10), and hepatic (Huh7) cancer cell lines (Fig. 2, C–E), as well as in cell lines from lymphoid origin, including a B acute lymphoblastic leukemia (BALL) cell line (Fig. 2 F) and T lymphocyte–derived Jurkat cells (Fig. 2 G).

CHOP binds the *Ulbp1* promoter to increase *Ulbp1* transcription

We investigated the mechanisms of *Ulbp1* transcription in ER-stressed cells. Consistent with previous studies (Kaser et al., 2008), we confirmed the activation of inositol requiring enzyme 1α (IRE1α; encoded by *Ern1*) and the RNA-activated protein kinase–like ER kinase pathway as shown by increased activating transcription factor 4 (ATF4) and CHOP expression in primary IECs from $Xbp1^{T\text{-}\Delta IEC}$ mice (Fig. S1 E). To determine which of these factors was associated with MULT1 induction, shCtrl or *shXbp1* MODE-K cells were co-silenced for IRE1α (*siErn1*), ATF4 (*siAtf4*), or CHOP (*siDdit3*), and MULT1 expression was analyzed by flow cytometry. The efficiency of siRNA silencing was determined

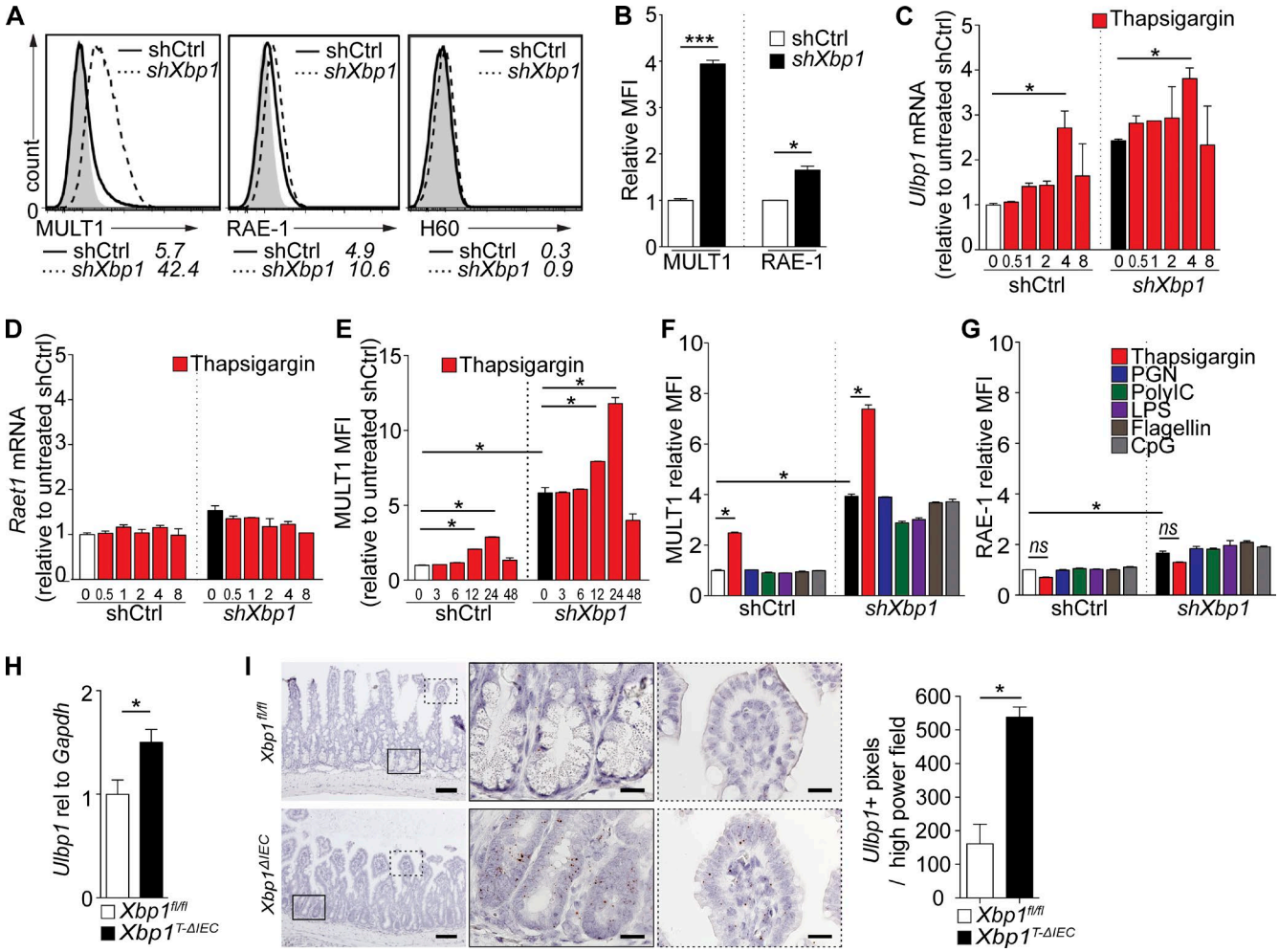

Figure 1. **ER stress results in up-regulation of MULT1 in vitro and in vivo.** (A) Representative histograms of NKG2D ligands on shCtrl and *shXbp1* MODE-K cells by flow cytometry (one of two independent experiments). (B) Knockdown of *Xbp1* in MODE-K cells results in significantly increased surface expression of MULT1 and RAE-1 as measured by increased mean fluorescent intensity (MFI) on MODE-K cells (one of two independent experiments). (C and D) Generalized ER stress, by administration of Tg, similarly increases mRNA expression of *Ulbp1* (C) but not *Raet1* (D) in shCtrl and *shXbp1* MODE-K cells (one of two independent experiments). (E) In line with this, MULT1 cell-surface expression increased significantly after Tg stimulation of shCtrl and *shXbp1* MODE-K cells (one of two independent experiments). (F and G) Increase in MULT1 surface expression (F) but not RAE-1 surface expression (G) occurs specifically in response to Tg-induced ER stress in MODE-K but not in response to treatment with a variety of TLR ligands (one of two independent experiments). CpG, CpG oligodeoxynucleotides; PGN, peptidoglycan; PolyIC, polyinosine-polycytidylic acid. (H) *Ulbp1* mRNA expression is increased in small intestinal crypt isolations of mice with deletion of *Xbp1* ($Xbp1^{\Delta IEC}$) in IECs, as compared with wild-type mice ($Xbp1^{fl/fl}$; $n = 6$ and $n = 4$, respectively). rel, relative. (I) Increased *Ulbp1* mRNA in small IECs of the $Xbp1^{\Delta IEC}$ mouse compared with the $Xbp1^{fl/fl}$ mouse ($n = 4$ per group). Bars: (low magnification) 100 µm; (high magnification) 20 µm. *, $P < 0.05$; ***, $P < 0.001$. All data represent mean ± SEM.

by immunoblotting and qPCR (Fig. S1, F and G). *siDdit3*, but not *siErn1* or *siAtf4*, transfection of *shXbp1* MODE-K cells reversed the increased MULT1 protein and mRNA expression (Fig. 3, A and B) observed in *shXbp1* MODE-K cells, suggesting that CHOP is involved in the induction of MULT1. Because CHOP functions as a transcription factor, we examined whether CHOP could directly regulate *Ulbp1* transcription. The 5′-flanking region (−267 to −257) of the *Ulbp1* gene has a similar sequence to a known CHOP-binding element, PuPuPuTGCAAT(A/C)CCC (Ubeda et al., 1996). Chromatin immunoprecipitation (ChIP) with an anti-CHOP antibody revealed evidence of increased direct CHOP binding to the promoter region of *Ulbp1* in *shXbp1* and Tg-stimulated MODE-K cells (Fig. 3 C). A reporter assay using luciferase reporter vectors was created to investigate the 5′-flanking region (−1,464 to 0) of the *Ulbp1* gene and demonstrated that a region between −447 and 0 contained the majority of CHOP-induced transcriptional activation of *Ulbp1* (Fig. 3 D). To confirm this mechanism for MULT1 induction in vivo, $Ddit3^{-/-}$ mice were crossed with $V\text{-}cre^{+};Xbp1^{fl/fl}$ mice to generate $Ddit3^{-/-};V\text{-}cre^{+};Xbp1^{fl/fl}$ mice ($Ddit3^{-/-};Xbp1^{\Delta IEC}$). Whereas *Ulbp1* mRNA

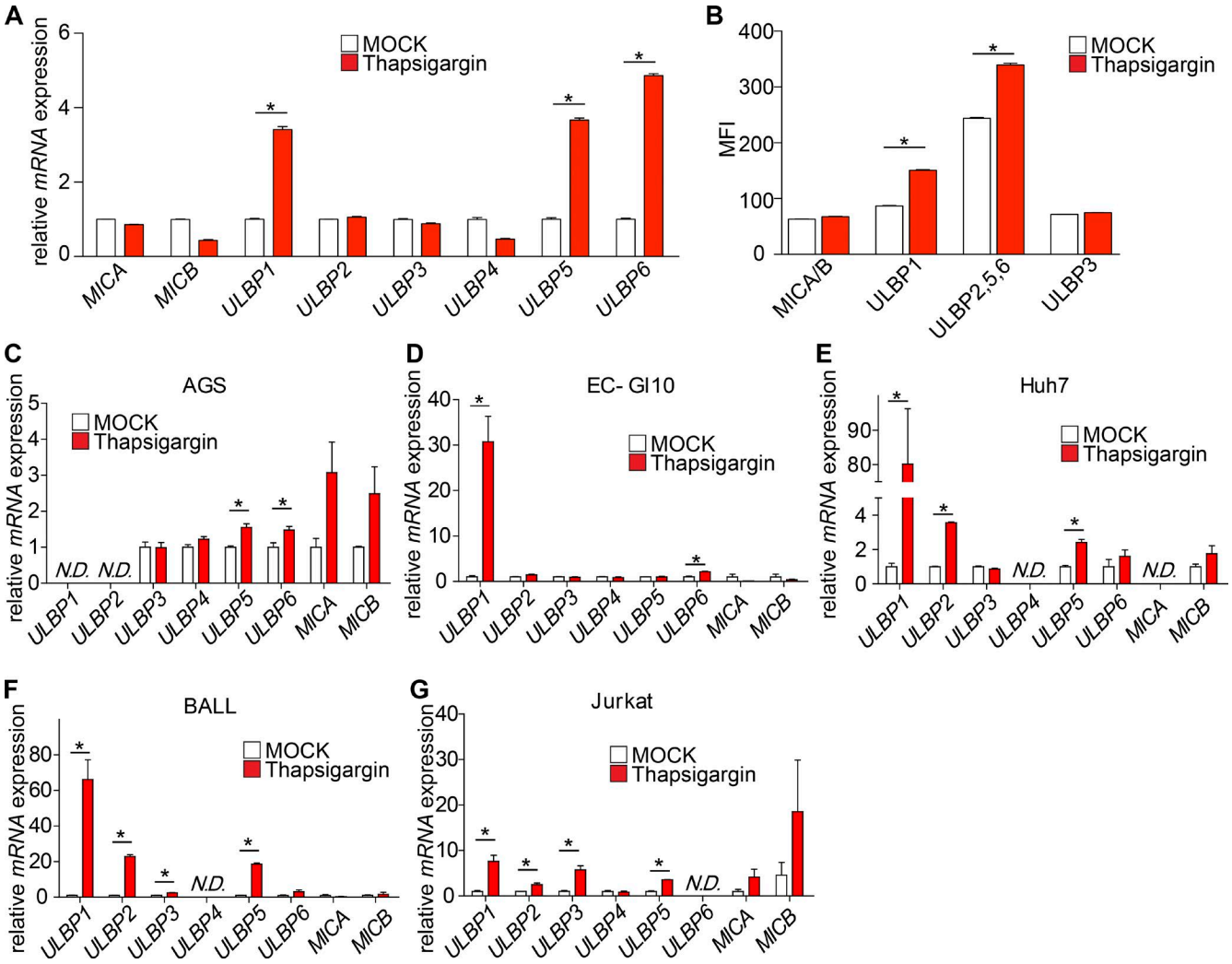

Figure 2. **ULBP up-regulation by ER stress on human cell lines.** (A and B) NKG2DL mRNA (A) and protein (B) expression in the human colorectal cancer cell line (HT29) by qPCR (A) or flow cytometry (B) after MOCK (DMSO) or Tg stimulation for 4 h (A) or 24 h (B). MFI, mean fluorescence intensity. (C–G) NKG2DL mRNA expression of AGS (C), EC-GI10 (D), Huh7 (E), BALL (F), and Jurkat (G) cell lines after MOCK or Tg stimulation for 4 h. *, $P < 0.05$. All data represent mean ± SEM. Representative plots are of at least two independent experiments.

expression was increased in crypt epithelial cells from *Xbp1*$^{\Delta IEC}$ mice in comparison with their littermate wild-type controls, up-regulation of *Ulbp1* mRNA expression was not observed in *Xbp1*$^{\Delta IEC}$ mice when CHOP was deficient, as observed in *Ddit3*$^{-/-}$;*Xbp1*$^{\Delta IEC}$ mice or their *Ddit3*$^{-/-}$ littermate controls (Fig. 3 E).

NKG2D-dependent, ER stress–induced inflammation is innate in nature

Given the strong and ER stress–specific up-regulation of NKG2DL on epithelial cells, we hypothesized that this could be a mechanism by which ER-stressed IECs are recognized by immune cells expressing the NKG2DL receptor NKG2D to allow for selective killing of stressed cells. To test this, we first treated *Xbp1*$^{T\text{-}\Delta IEC}$ mice with a neutralizing, nondepleting anti-NKG2D antibody and demonstrated that, indeed, blockade of NKG2D–NKG2DL interactions diminished ER stress–induced inflammation (Fig. 4 A). Then, we focused on intestinal intraepithelial lymphocytes (IELs [iIELs]), which have been proposed to provide for local and directed immune responses against IECs that are altered by environmental agents, infections, or neoplastic transformation (Rhodes et al., 2008). We investigated the subsets that have been described to express NKG2D, including various T cell subsets and NK cells (Raulet, 2003), using the gating strategy described in Fig. 4 B and Fig. S2.

Although small iIELs from *Xbp1*$^{T\text{-}\Delta IEC}$ mice did not contain higher frequencies of T cells and showed a trend toward lower overall frequencies of $\alpha\beta^+$ T cells, we observed a significant increase in $\gamma\delta^+$ T cells (Fig. 4 C). As intraepithelial

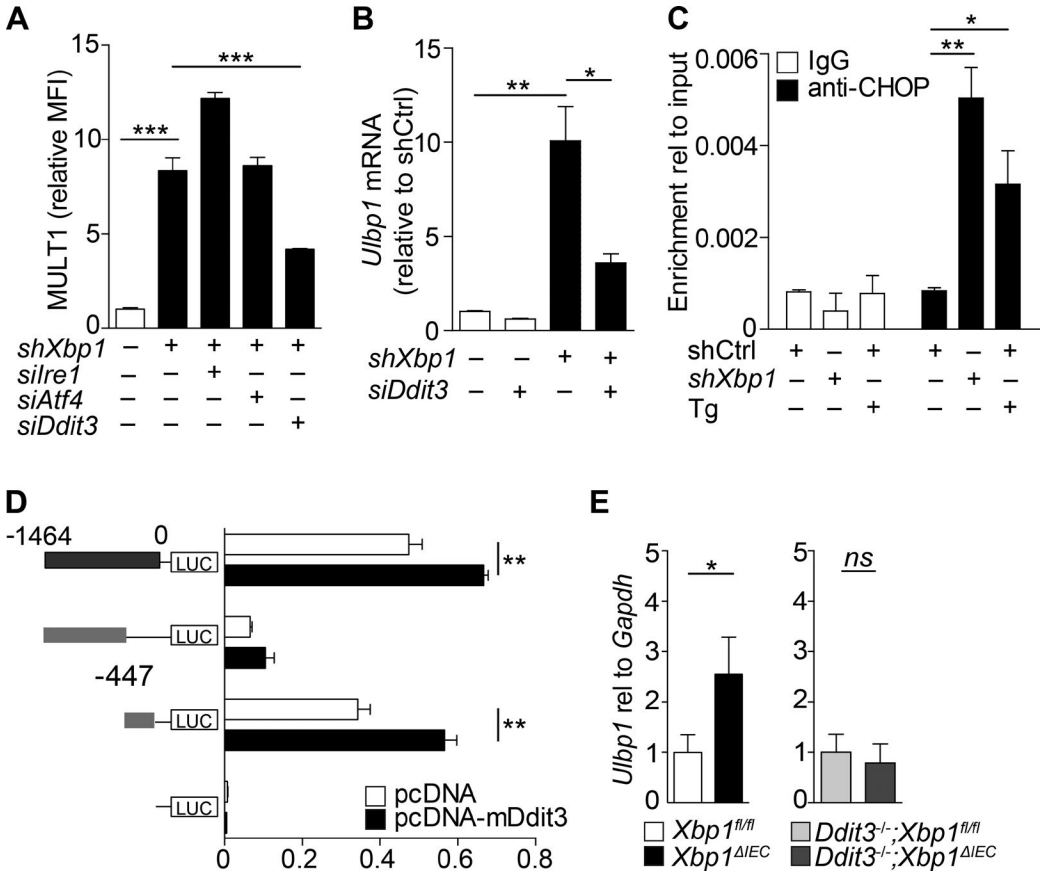

Figure 3. **CHOP binds the *Ulbp1* promotor and is important for ER stress–induced up-regulation of *Ulbp1*.** (A) Whereas co-silencing of IRE1α or ATF4 did not have an effect on MULT1 surface expression on *shXbp1* MODE-K cells, as compared with shCtrl, co-silencing with *siDdit3* significantly decreased MULT1 mean fluorescence intensity (MFI; one of two independent experiments). (B) In line, *siDdit3* significantly decreased *Ulbp1* mRNA expression in MODE-K (one of two independent experiments). (C) qPCR for predicted MULT1 promoter sequence after anti-CHOP ChIP. shCtrl with/without Tg stimulation or *shXbp1* MODE-K cells were analyzed (one of two independent experiments). rel, relative. (D) Firefly luciferase (LUC) reporter plasmids, including the *Ulbp1* promoter regions with CHOP expression plasmid (pcDNA-mDdit3) or empty plasmid (pcDNA), were cotransfected into shCtrl MODE-K cells. Luciferase activity was measured and normalized against Renilla luciferase activity (one of two independent experiments). (E) *Ulbp1* mRNA expression in mucosal scraping is not increased in $Ddit3^{-/-};Xbp1^{\Delta IEC}$ double-mutant mice as opposed to $Xbp1^{\Delta IEC}$ single-knockout mice (n = 7–12 per group). *, P < 0.05; **, P < 0.01; ***, P < 0.001. All data represent mean ± SEM.

γδ$^+$ T cells can express NKG2D (Ono et al., 2012), we investigated NKG2D expression on γδ$^+$ T cells and found significantly increased levels of NKG2D on γδ$^+$ T cells in $Xbp1^{T\text{-}\Delta IEC}$ mice (Fig. 4 D). However, γδ$^+$ T cells did not significantly contribute to the spontaneous inflammation of $Xbp1^{\Delta IEC}$, as $Tcrd^{-/-};V\text{-}cre^{+};Xbp1^{fl/fl}$ ($Tcrd^{-/-};Xbp1^{\Delta IEC}$) mice lacking γδ$^+$ T cells (Shiohara et al., 1996) did not exhibit lower levels of enteritis as compared with $Xbp1^{\Delta IEC}$ mice (Fig. 4 E). Consistent with this, transcriptional analysis of γδ$^+$ cells obtained from the intestinal epithelium of $Xbp1^{\Delta IEC}$ mice did not reveal evidence of inflammatory and cytotoxic potential when compared with those isolated from wild type (Fig. S3).

Then, we investigated whether the adaptive immune system was at all required for the development of inflammation in response to ER stress in the small intestinal epithelium by crossing $Rag1^{-/-}$ with $Xbp1^{\Delta IEC}$ mice. Interestingly, $Rag1^{-/-};Xbp1^{\Delta IEC}$ mice developed spontaneous enteritis that was similar to the enteritis observed in $Xbp1^{\Delta IEC}$ mice (Fig. 4 F), and histological characteristics of ER stress, including hypomorphic Paneth cells and goblet cells (Fig. S4 A), were similar to that observed in $Xbp1^{\Delta IEC}$ mice, as previously described (Kaser et al., 2008; Adolph et al., 2013). Moreover, both pathological severity and kinetics of onset were comparable between $Rag1^{-/-};Xbp1^{\Delta IEC}$ mice and $Xbp1^{\Delta IEC}$ mice (Fig. 4 G). These results demonstrate that, although the adaptive immune system may play a role in chronic ER stress–induced inflammation (Eri et al., 2011), it is not required for the development of inflammation in $Xbp1^{\Delta IEC}$ mice.

Intraepithelial ILCs contribute to the development of ER stress–induced inflammation in an NKG2D-dependent manner

We focused our attention on NK cells, gated as CD45$^+$CD3$^-$CD19$^-$ NKp46$^+$NK1.1$^+$ cells (Fig. 5 A and Fig.

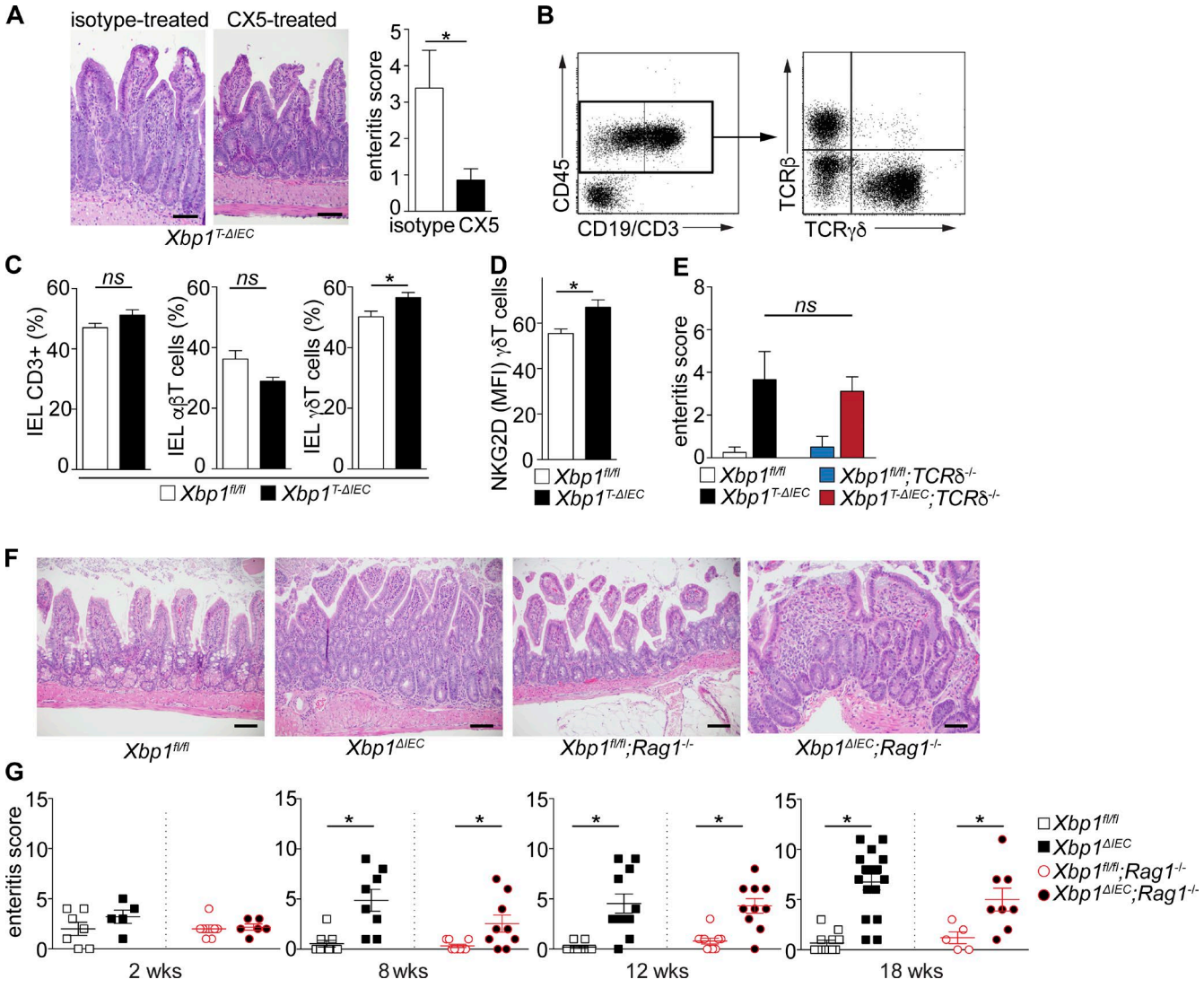

Figure 4. **NKG2D-dependent ER stress–induced intestinal inflammation does not require an adaptive immune system.** (A) Development of enteritis in *Xbp1*$^{T\text{-}\Delta IEC}$ mice is significantly inhibited by treatment with anti-NKG2D antibody (CX5), as compared with isotype-matched control Ig (n = 13–14 per group). Representative H&E staining of the experimental group is shown. Bars, 100 µm. (B and C) Flow cytometric analysis of iIELs from *Xbp1*$^{fl/fl}$ and *Xbp1*$^{T-\Delta IEC}$ mice for CD3$^+$ cells, αβT cells, and γδ T cells (n = 4 per group). (D) NKG2D expression is significantly increased on IEL-γδ T cells from *Xbp1*$^{T-\Delta IEC}$ mice (n = 4 per group). MFI, mean fluorescence intensity. (E) Enteritis scores of *Xbp1*$^{fl/fl}$, *Xbp1*$^{\Delta IEC}$, *Xbp1*$^{fl/fl}$;*Tcrd*$^{-/-}$, and *Xbp1*$^{\Delta IEC}$;*Tcrd*$^{-/-}$ demonstrate that γδ T cells are not required for ER stress–induced inflammation (n = 4–9 mice per group). (F) H&E staining of 12-wk-old *Xbp1*$^{fl/fl}$, *Xbp1*$^{\Delta IEC}$, *Rag1*$^{-/-}$*Xbp1*$^{fl/fl}$, and *Rag1*$^{-/-}$*Xbp1*$^{\Delta IEC}$ mice shows normal histology in *Xbp1*$^{fl/fl}$ and *Rag1*$^{-/-}$*Xbp1*$^{fl/fl}$. Enteritis is observed in both *Xbp1*$^{\Delta IEC}$ and *Rag1*$^{-/-}$*Xbp1*$^{\Delta IEC}$ mice (representative H&E of experimental groups). Bars, 100 µm. (G) Enteritis scores of *Rag1*$^{-/-}$, *Xbp1*$^{\Delta IEC}$ double-mutant mice compared with *Xbp1*$^{\Delta IEC}$ shows similar onset and kinetics of inflammation (n = 5–16 per group). *, P < 0.05. All data represent mean ± SEM.

S2 B). This population expressed intranuclear eomesodermin (EOMES) but not surface IL-7 receptor subunit α (IL7Ra; Fig. S4, B and C), identifying this population as intraepithelial group 1 ILCs, which consist of conventional NK cells and ILC1. Indeed, we observed a significant increase of the group 1 ILCs that expressed NKG2D and CD25 as a sign of their activation status in response to ER stress (Fig. 5 B and Fig. S2 D). Similarly, and in line with our hypothesis that the group 1 ILCs mediate inflammation, increased frequencies of intraepithelial group 1 ILCs, expressing higher levels of NKG2D, were observed in *Rag1*$^{-/-}$*;Xbp1*$^{\Delta IEC}$ mice (Fig. 5 C). Although we found evidence for the presence of intraepithelial innate-like NK1.1$^+$CD3$^+$ T cells (Zeissig et al., 2007; Haas et al., 2009), a fraction of which expressed NKG2D, we observed that the expression levels of NKG2D did not differ between *Xbp1*$^{fl/fl}$ and *Xbp1*$^{\Delta IEC}$ mice (Fig. S4, D and E).

To study NKG2D-mediated killing of ER-stressed IECs, we co-cultured *shXbp1* MODE-K cells with splenic

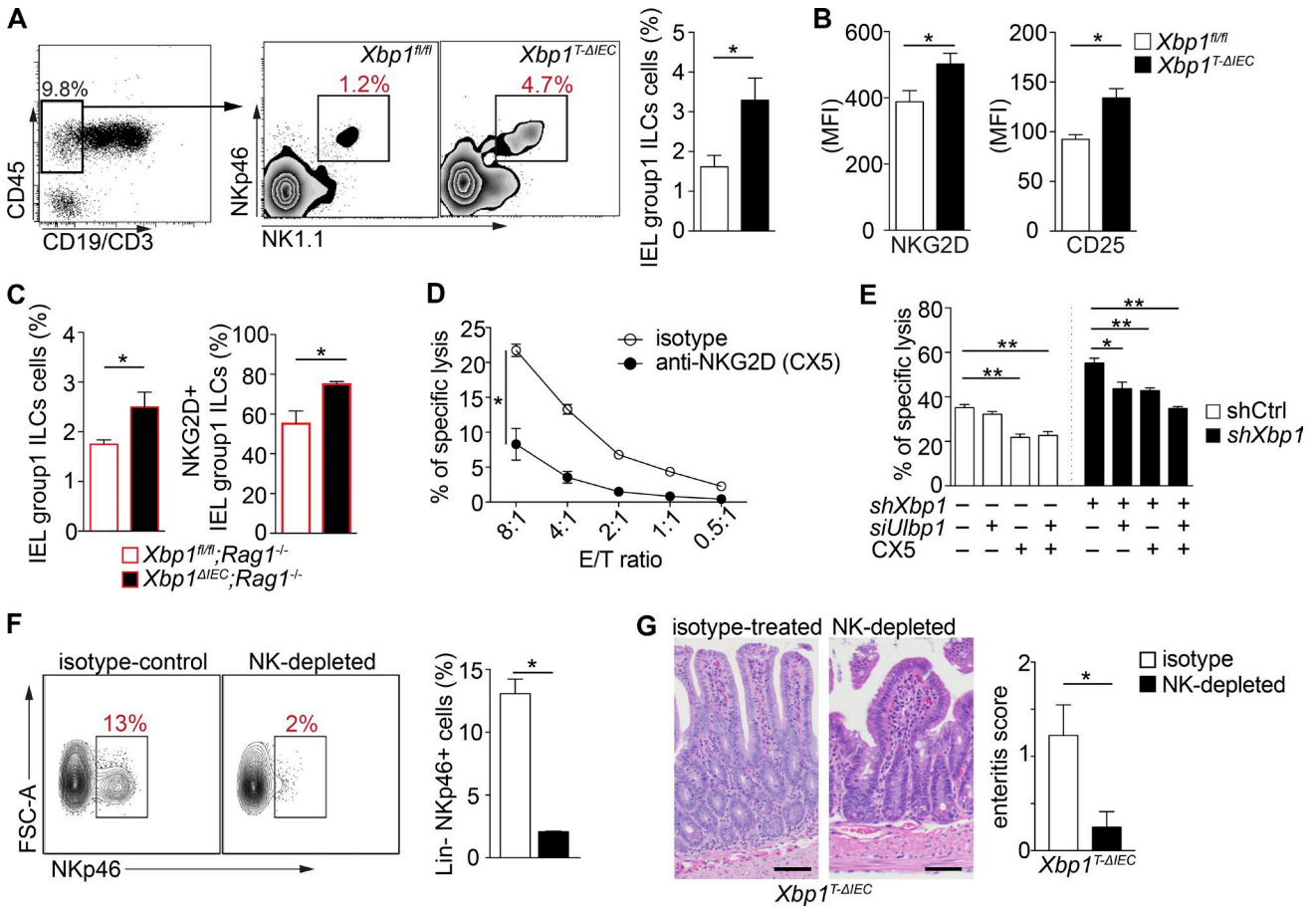

Figure 5. **Intraepithelial group 1 ILCs play a key role in the development of intestinal inflammation in response to ER stress.** (A) Flow cytometric analysis of IEL group 1 ILCs from *Xbp1*$^{fl/fl}$ and *Xbp1*$^{T-\Delta IEC}$ mice (one of two independent experiments). (B) NKG2D and CD25 expression on IEL group 1 ILCs in *Xbp1*$^{fl/fl}$ and *Xbp1*$^{T-\Delta IEC}$ mice (n = 4 mice per group). MFI, mean fluorescence intensity. (C) Frequency of IEL group 1 ILCs in *Xbp1*$^{fl/fl}$;*Rag1*$^{-/-}$ and *Xbp1*$^{\Delta IEC}$;*Rag1*$^{-/-}$ (n = 4 mice per group). (D) CFSE-labeled MODE-K cells were incubated for 4 h with primary splenic NK cells preactivated by recombinant IL-2. Cytotoxicity was assessed by flow cytometry after 7-AAD staining. NK cells were pretreated with anti-NKG2D–blocking antibody (CX5) or isotype-matched control Ig for 30 min before incubation at the indicated E:T ratios (depicted is one of two independent experiments). (E) NK cells, pretreated with anti-NKG2D (CX5) or isotype-matched control Ig, were used as effector cells. shCtrl and *shXbp1* MODE-K cells co-silenced with *Ulbp1* or control siRNA were used as target cells. The E:T ratio was 16:1 (depicted is one of two independent experiments). (F) Flow cytometry of CD3$^-$NKp46$^+$ IELs shows efficient depletion of IEL group 1 ILCs (n = 4 per group). FSC, forward scatter. (G) Depletion of IEL group 1 ILCs inhibits the development of inflammation in of *Xbp1*$^{T-\Delta IEC}$ mice (representative H&E staining of experimental groups; bars, 50 µm; n = 8–9 mice per group). Representative H&E staining of the indicated treatments is shown. *, P<0.05; **, P<0.01. All data represent mean ± SEM.

NK cells and demonstrated that pretreatment of NK cells with a blocking anti-NKG2D antibody significantly decreased specific lysis in vitro (Fig. 5 D). Similarly, silencing of *Ulbp1* with *siUlbp1* decreased NK cell–mediated specific lysis of *shXbp1* MODE-K cells, and this effect was further enhanced by co-treatment with anti-NKG2D antibody (Fig. 5 E). Furthermore, IELs from *Xbp1*$^{\Delta IEC}$ mice were more cytolytic, as they exhibited increased killing of MULT1-transfected RMA cells, a mouse T cell lymphoma cell line, in comparison with the activity observed with IELs from wild-type (*Xbp1*$^{fl/fl}$) mice (Fig. S5). To determine the importance of intraepithelial group 1 ILCs in the development of small intestinal enteritis in vivo, we treated *Xbp1*$^{T-\Delta IEC}$ mice with antibodies to deplete NK1.1$^+$ cells and demonstrated that this resulted in a significant depletion of intraepithelial group 1 ILCs defined as CD45$^+$CD3$^-$NKp46$^+$ cells (Fig. 5 F; Sips et al., 2012). Consistent with our observations in the co-culture system in vitro, NK1.1$^+$ cell–depleted *Xbp1*$^{T-\Delta IEC}$ mice exhibited significantly reduced enteritis scores as compared with isotype-matched control Ig-treated animals (Fig. 5 G), further demonstrating that intraepithelial group 1 ILCs, and potentially innate-like NK1.1$^+$ T cells when an adaptive immune system is present, play a key role in the development of ER stress–induced inflammation.

DISCUSSION

Here, we demonstrate that ER stress in the intestinal epithelium drives spontaneous small intestinal enteritis and can

occur in the presence of only an innate immune system. Furthermore, ER stress in IECs is sensed by their increased surface expression of NKG2DLs that are recognized by intestinal NKG2D-expressing intraepithelial group 1 ILCs (NK cells and ILC1) and potentially innate-like T cells, if an adaptive immune system is present.

It has long been known that iIELs in the small intestine represent a complex collection of lymphocytes, which includes $\alpha\beta^+$ T cells that are either $CD8\alpha\alpha^+$ or $CD8\alpha\beta^+$, $\gamma\delta^+$ T cells, innate-like T cells (Wencker et al., 2014), and ILCs, which includes NK cells and ILC1. Intraepithelial NK cells that are $CD45^+CD3^-NKp46^+$ (Sips et al., 2012) and display IFN-γ production and cytotoxic activity have been previously described in mice (Tagliabue et al., 1982; Keilbaugh et al., 2005) and humans (León et al., 2003). It has also recently been recognized that ILC1 can be detected within the small intestinal epithelium (Robinette et al., 2015) and is increased in Crohn's disease in humans (Fuchs et al., 2013). Although the exact relationship between classical NK cells and ILC1s in the small intestinal epithelium remains controversial, particularly in the setting of inflammation, it is interesting to note that intraepithelial ILC1s are phenotypically similar to NK cells (Bernink et al., 2015; Spits et al., 2016). Thus, our experiments suggest that ER stress in IECs may be an important factor in the accumulation and function of intraepithelial group 1 ILCs that are observed in inflammatory bowel disease and potentially other inflammatory conditions.

NKG2D ligands are MHC class I–like molecules, which include mouse RAE-1, MULT1, and H60, whose human equivalents are MHC class I chain-related gene A (MICA), MICB, and ULBP 1–6 (Champsaur and Lanier, 2010; Lanier, 2015). As early as 7 d after tamoxifen-induced *Xbp1* deletion in IECs in vivo, we observed specific induction of *Ulbp1* but surprisingly not *Raet1* or *H60*. NKG2D ligands can be transcriptionally induced by various types of cell stress, including DNA damage through ATM (ataxia telangiectasia; mutated) or ATR (ATM and Rad3 related) protein kinases (Gasser et al., 2005), TLRs (Hamerman et al., 2004; Ebihara et al., 2007; Chen et al., 2011a), heat shock (Groh et al., 1996), and oxidative stress (Venkataraman et al., 2007), and have recently also been linked to ER stress in the setting of cancer (Gowen et al., 2015). In the latter study, ATF4 was identified as a critical protein involved in ULBP1 transcription and surface expression. Interestingly, ATF4 appeared to be particularly important for the induction of ULBP1, but not other NKG2DLs, showing a similar specificity of ER stress–induced NKG2DL as reported here. In contrast, however, we did not identify a role for ATF4 in the induction of MULT1 as deduced from silencing *Atf4* expression in *shXbp1* MODE-K cells. There are several possible explanations. In our studies, we used an immortalized, but not transformed, IEC line (Vidal et al., 1993). In addition, although knockdown of *Atf4* using *siAtf4* was efficient, CHOP levels were still observed to be increased in response to Tg. This is consistent with the fact that, although ATF4 is a critical regulator of CHOP, it has been described that the *Chop* promoter contains binding sites for ATF6 and XBP1 as well and could in that way be induced independently of ATF4 by Tg-induced ER stress (Kim et al., 2008).

NKG2D is a type II transmembrane-anchored C-type lectin-like activating receptor that is expressed by NK cells, activated $CD8^+$ T cells, NKT cells, subsets of $\gamma\delta^+$ T cells, innate-like T cells, and $CD4^+$ T cells (Champsaur and Lanier, 2010; Fuchs et al., 2013; Wencker et al., 2014; Lanier, 2015). When NKG2D binds its ligands, it promotes immune responses against infected or neoplastic cells, triggering cell-mediated cytotoxicity and secretion of cytokines (e.g., IFN-γ) and chemokines (Champsaur and Lanier, 2010; Lanier, 2015). In Celiac disease, stress-inducible MICA molecules trigger direct activation of intraepithelial T cells via NKG2D, allowing for the killing of IECs (Hüe et al., 2004). A recent proof-of-concept clinical trial of a single dose of blocking anti-NKG2D (NNC0142-0002) IgG_4 monoclonal antibody in patients with moderately to severely active Crohn's disease supports the importance of NKG2D in the pathogenesis of intestinal inflammation (Allez et al., 2016). Indeed, we found that, in the setting of intestinal epithelial ER stress, NKG2D expression on immune cells and especially intraepithelial group 1 ILCs was an important component of innate immune activation, as demonstrated by the decreased enteritis observed upon pharmacological blockade of NKG2D and depletion of NK1.1-expressing cells and the presence of inflammation in $Rag1^{-/-}Xbp1^{\Delta IEC}$ double-mutant mice.

In summary, we show that IEC-associated ER stress uniquely results in selective up-regulation of MULT1 in mice and human ULBP-related protein in a pathway that involves CHOP. CHOP transcriptionally regulates these, but not other, NKG2DLs resulting in increased NKG2D-mediated epithelial cytolysis. As CHOP has also been shown to activate death receptor 5 resulting in cell apoptosis (Lu et al., 2014), our observations further suggest that CHOP is a critical factor in linking ER stress to innate immune responses. Specifically, we demonstrate that up-regulation of MULT1 is linked to the activity of intraepithelial group 1 ILCs, which promotes spontaneous enteritis in an NKG2D-mediated pathway that might also involve innate-like T cells if an adaptive immune system is present. Nonetheless, our studies further reveal a dispensable role of the adaptive immune system in the enteritis associated with epithelial-associated ER stress. Altogether, we define a pathway by which ER stress is linked to the specific up-regulation of particular NKG2DLs and suggest that the increased presence of group 1 ILCs in the epithelium during intestinal inflammation is reflective of a host immune response to ER stress at this site.

MATERIALS AND METHODS

Mice

$Xbp1^{fl/fl}$ (129;B6;BALB/c) mice were backcrossed eight times with C57BL/6 (B6) mice to obtain $Xbp1^{fl/fl}$ B6 transgenic mice, and $V\text{-}cre^+;Xbp1^{fl/fl}$ ($Xbp1^{\Delta IEC}$) B6 mice were obtained as described previously (Adolph et al., 2013). For the transient

Cre-mediated deletion of the floxed *Xbp1* gene, we mated *Xbp1*$^{fl/fl}$ B6 mice with *V-creER*^{T2} B6 mice, which were obtained by backcrossing *V-creER*^{T2} (129;B6) mice (provided by N. Davidson, Washington University in St. Louis, St. Louis, MO; and S. Robine, Institut Curie-Centre National de la Recherche Scientifique, Paris, France; El Marjou et al., 2004) eight generations onto the C57BL/6 background. Cre recombinase was activated by daily intraperitoneal administration of 1 mg tamoxifen (MP Biomedicals) in 100 µl of sunflower oil for 7 d, and mice were sacrificed the day after a final injection of tamoxifen. Sex- and age-matched littermate *V-cre*$^{-}$*;Xbp1*$^{fl/fl}$ mice were used as controls. All mice were genotyped by PCR of genomic DNA isolated from proteinase K–digested tail skin by phenol extraction and isopropanol precipitation. Primer sequences were as described previously (Adolph et al., 2013). The experiments were approved by the Harvard Standing Committee on Animals.

Hematoxylin and eosin (H&E) staining, periodic acid–Schiff (PAS)–Alcian blue staining, and histology

Small intestinal tissues from mice were isolated using standard techniques and stained with H&E as previously described (Adolph et al., 2013). Goblet cells and Paneth cells were stained with PAS–Alcian blue dye using an Alcian blue/PAS staining kit (Newcomer Supply) according to the manufacturer's instruction. A semiquantitative composite scoring system was used for the assessment of spontaneous intestinal inflammation, calculated as a sum of four histological subscores: mononuclear cell infiltration (0, absent or normal sparse lymphocytic infiltration; 1, mild or diffuse increase in lamina propria; 2, moderate or lamina propria increased with basal localization aggregates displacing crypts; and 3, severe or lamina propria with submucosal infiltration), crypt hyperplasia (0, absent; 1, mild; 2, moderate; and 3, severe), epithelial injury/erosion (0, absent; 1, mild or crypt dropout or surface epithelial damage without frank erosion or ulceration; 2, moderate or focal ulceration; and 3, severe or multifocal or extensive ulceration), and polymorphonuclear cell infiltration (0, absent; 1, mild or lamina propria only; 2, moderate or lamina propria infiltration with cryptitis or crypt abscesses; and 3, severe or sheet-like or submucosal infiltration). Scores were multiplied by a factor based on the extent of the inflammation. The extent factor was derived according to the fraction of bowel length involved by inflammation: 1, 10%; 2, 10–25%; 3, 25–50%; and 4, 50%. The score was assessed by an expert gastrointestinal pathologist (J.N. Glickman) who was blinded to the genotype and experimental conditions of the samples.

Immunohistochemistry and RNA in situ hybridization

Formalin-fixed paraffin-embedded tissue sections were stained by standard immunohistochemistry using a VECTAS TAIN ABC kit (Vector Laboratories) and DAB Peroxidase Substrate kit (Vector Laboratories) according to the manufacturer's instructions. For RNA in situ hybridization, 5-µm formalin-fixed, paraffin-embedded tissue sections were processed using the RNAscope 2.5 HD Assay and Mm-Ulbp1 probe (target region 2–1,472; Advanced Cell Diagnostics) according to the manufacturer's instructions. The *Ulbp1*$^{+}$ signals by in situ hybridization were counted as pixels per high-power field using ImageJ software (National Institutes of Health).

Cell culture

The SV40 large T-antigen–immortalized small IEC line MODE-K (gift from D. Kaiserlian, Institute Pasteur, Paris, France) was maintained in DMEM supplemented with 10% FCS, 2 mM L-glutamine, nonessential amino acid, sodium pyruvate, 100 U/ml penicillin, and 100 µg/ml streptomycin (DMEM10; Vidal et al., 1993). The MODE-K cells were transduced with *Xbp1*-specific (*shXbp1*) or control shRNA lentiviral vectors and selected with hygromycin (GIBCO) to establish stable clones as described previously (Adolph et al., 2013). The shCtrl and *shXbp1* MODE-K cells were co-silenced for *Ern1*, *Atf4*, *Ddit3*, or *Ulbp1* using siRNA or scrambled control (Ambion). The human gastric cancer cell line AGS;NCI-N87 (American Type Culture Collection), as well as the human B cell leukemia cell line BALL-1;RCB0256 (Institute of Physical and Chemical Research Gene Bank) and the human T cell leukemia cell line Jurkat;TIB-152 (American Type Culture Collection), were cultured in RPMI-1640 medium supplemented with 10% FCS.

The human hepatocellular carcinoma cell line Huh7; JCRB0403 (Japanese Collection of Research Bioresources) was cultured in DMEM supplemented with 10% FCS, and the cell line EC-GI-10;RCB0774 (Institute of Physical and Chemical Research Gene Bank) was maintained in HamF12 supplemented with 10% FCS. All in vitro experiments were performed in duplicate or triplicate.

Antibodies and reagents

Anti–β-actin (Sigma), anti-CHOP, IRE1α (Cell Signaling Technology), anti-ATF4, and anti-ATF6 (Santa Cruz Biotechnology) were used for immunoblotting. Fluorescence-conjugated antibodies against CD3 (clone 17A2), CD4 (RM4-5), CD8 (53-6.7), CD19 (6D5), CD25 (PC61), CD45 (30-F11), NK1.1 (PK136), NKp46 (29A1.4), NKG2D (CX5), Ly49-C/I/F/H (14B11), TCRβ (H57-597), TCRγδ (GL-3), RORγt (AFKJS-9), EOMES (Dan11mag), $H2K^{b}$ (AF6-88.5), $H2K^{k}$ (36-7-5), MULT1 (237104), RAE-1 (186107), H60 (205326), MICA/B (159207), ULBP1 (170818), ULBP2/5/6 (165903), and ULBP3 (166510) were purchased from BD Biosciences, eBioscience, BioLegend, or R&D systems (Minneapolis). Anti-lysozyme (DAKO) antibody was used for primary antibodies in immunohistochemistry. For blocking NKG2D receptor, rat anti–mouse NKG2D mAb was purified from hybridoma (clone CX5) supernatant. To efficiently deplete group 1 ILCs in the intestinal intraepithelial compartment, anti–mouse NK1.1 mAb (clone PK136; BioLegend) and rabbit anti–asialo ganglio–*N*-tetraosylceramide (asialo-GM1) antisera (Wako Chemicals) were used. Tg (Sigma) and tunicamycin (Sigma) were dissolved in DMSO as recommended by the manufacturer.

RNA isolation and qPCR

RNA samples were extracted and purified using an RNeasy Mini kit (Qiagen), and complementary DNAs were synthesized using SuperScript III (Life Technologies). Real-time RT-PCR was performed using a LightCycler 480 SYBR Green I Master (Roche) and a CFX96 Real-Time (Bio-Rad) system. Values were normalized to the expression of *Gapdh* for each sample. Primers used for qPCR were as follows: for *Ulbp1*, 5′-CTAACACAACCGGAAAGCCCCT-3′ and 5′-CAGTGCTTGTGTCAACACGGA-3′ or 5′-GCAGGC TGAGGTGTGTGGCC-3′ and 5′-CCAGGTCCTGCA GTCGCCCT-3′ (Chen et al., 2011b); *Raet1*, 5′-TCCGCA AAGCCAGGGCCAAA-3′ and 5′-GCTGGTAGGTGG AAGCGGGG-3′ (Chen et al., 2011b); *H60*, 5′-GTGTGA TGACGATTTGTTGAG-3′ and 5′-ATTGATGGATTC TGGGCCATC-3′ (Rabinovich et al., 2003); *Xbp1*, 5′-AGC AGCAAGTGGTGGATTTG-3′ and 5′-GAGTTTTCT CCCGTAAAAGCTGA-3′ (Wang and Seed, 2003); *Xbp1s*, 5′-ACACGCTTGGGAATGGACAC-3′ and 5′-CCATGG GAAGATGTTCTGGG-3′ (Iwakoshi et al., 2003); *Ddit3*, 5′-CTGGAAGCCTGGTATGAGGAT-3′ and 5′-CAGGGT CAAGAGTAGTGAAGGT-3′ (Wang and Seed, 2003); Ifng, 5′-TCAGCAACAGCAAGGCGAAAAAGG-3′ and 5′-CCACCCCGAATCAGCAGCGA-3′ (Olszak et al., 2014); Gzmb, 5′-TCTTGACGCTGGGACCTAGGCG-3′ and 5′-GGGCTTGACTTCATGTCCCCCG-3′; Il17a, 5′-CTC CCTTGGCGCAAAAGTGAGCT-3′ and 5′-ATTGCG GTGGAGAGTCCAGGGT-3′; and Nkg2d, 5′-CGACCT CAAGCCAGCAAAGTG-3′ and 5′-TGTTGCTGAGAT GGGTAATG-3′. Primers for the human cell line were as follows: for *MICA*, 5′-CCTTGGCCATGAACGTCAGG-3′ and 5′-CCTCTGAGGCCTCGCTGCG-3′; *MICB*, 5′-ACCTTGGCTATGAACGTCACA-3′ and 5′-CCCTCT GAGACCTCGCTGCA-3′; *ULBP1*, 5′-CAAGTGGAG AATTTAATACCCATTGAG-3′ and 5′-TGTTGTTTG AGTCAAAGAGGA-3′; *ULBP2*, 5′-TTACTTCTCAAT GGGAGACTGT-3′ and 5′-TGTGCCTGAGGACATGGC GA-3′; *ULBP3*, 5′-CCTGATGCACAGGAAGAAGAG-3′ and 5′-TATGGCTTTGGGTTGAGCTAAG-3′; *ULBP4*, 5′-CCTCAGGATGCTCCTTTGTGA-3′ and 5′-CGA CTTGCAGAGTGGAAGGATC-3′; *ULBP5*, 5′-TGGCCG ACCCTCACTCTCT-3′ and 5′-CCGTGGTCCAGGTCT GAACT-3′; and ULBP6, 5′-AATCTCTTGTCCCCAGCC CT-3′ and 5′-GTGAGGGTCGTCTCGCCTA-3′.

Flow cytometry

IECs and iIELs were isolated as described previously (Olszak et al., 2014). In brief, fat and Peyer's patches were removed from collected small intestines, and then the intestines were cut longitudinally and washed in PBS. After removing mucus by treatment with 1 mM dithiothreitol in PBS for 15 min at room temperature, intestines were disrupted by shaking in RPMI-1640 medium containing 20 mM Hepes and 5 mM EDTA for 30 min at 37°C. After filtering through a 100-µm strainer, cells were layered on a 40–75% Percoll gradient (GE Healthcare), IECs were isolated from the top layer, and iIELs were isolated from the cells at the 40–75% interface. After filtering through a 40-µm strainer, cells were stained with fluorescence-conjugated antibodies after incubation with anti-CD16+CD32 antibody for 15 min on ice. Flow cytometry was performed using a MACSQuant flow cytometer (Miltenyi Biotec) and analyzed using FlowJo software (TreeStar).

Intestinal epithelial scrapings and crypt isolation

Mice were sacrificed, and the intestines were collected, opened longitudinally, and washed with ice-cold PBS. Intestinal epithelium was collected by scraping with glass slides and snap frozen into liquid nitrogen for further analysis. For protein analysis, the intestinal epithelial scrapings were homogenized in radioimmunoprecipitation assay buffer (50 mM Tris [pH 7.4], 150 mM NaCl, 1% Nonidet P-40, 0.5% sodium deoxycholate, and 0.1% SDS) supplemented with protease inhibitor (Complete; Roche Applied Science) using a 25-G needle with a syringe. Lysates were cleared by centrifugation at 10,000 *g* for 15 min at 4°C and then assayed by standard immunoblotting by using specific antibodies as indicated in Results and the figure legends. For RNA analysis, RNA was extracted from the scraping by using an RNeasy Mini kit (Qiagen) according to the manufacturer's instructions. To isolate crypts from mouse small intestine, collected intestine was flushed by ice-cold PBS, cut longitudinally, and then incubated on ice for 30 min in 2 mM EDTA in PBS. Two sedimentation steps and application of a cell strainer separated crypts from villi, which were then used for RNA isolation (Qiagen).

ChIP

ChIP with rabbit anti-CHOP (Cell Signaling Technologies) and control IgG rabbit antibody (Cell Signaling Technologies) was performed in Xbp1 and control silenced MODE-K cells by using a SimpleChIP Plus Enzymatic ChIP kit (Cell Signaling Technologies). Immunoprecipitated DNA was subject to qPCR to determine enrichment of CHOP binding to respective promoters (−431 to −272 bp relative to the start codon of *Ulbp1*), and results were normalized to input chromatin DNA. Primers used for qPCR were as follows: forward, 5′-TGTAGATCACCCTACCCAGCCT-3′ and reverse, 5′-TAAGAAGGACTCGAAGTGCAGGA-3′.

Reporter assay

To generate Ulbp1-pGL3 firefly luciferase reporter plasmids, DNA fragments including the *Ulbp1* promoter regions −1,464 to 0, −1,464 to −427, and −447 to 0 bp relative to the start codon were amplified from mouse genomic DNA using primers: 5′-CCGGGGTACCTGAGAACATAGCAGAAC AGACCAG-3′ and 5′-CCGGGCTAGCAGCTGCTTCTC TAGACTCTGGC-3′, 5′-CCGGGGTACCTGAGAACA TAGCAGAACAGACCAG-3′ and 5′-CCGGGCTAGCCT ACAGAGCAAGCAGGAGCTC-3′, and 5′-CCGGGG TACCGAGCTCCTGCTTGCTCTGTAG-3′ and 5′-CCG GGCTAGCAGCTGCTTCTCTAGACTCTGGC-3′, re-

spectively. The PCR products were inserted into pGL3-Basic plasmid (Promega) between the *Kpn*I and *Nhe*I sites. To generate the mouse CHOP expression plasmid, cDNA encoding mouse CHOP corresponding to nucleotides 30–734 was amplified by PCR, using primers 5′-CCGGGAATTCCA TACACCACCACACCTGAA-3′ and 5′-CCGGAAGCT TTGTACCGTCTATGTGCAAGC-3′, and was inserted into pcDNA3.1(–) plasmid between *Eco*RI and *Hind*III. MODE-K cells were transfected with 50 ng of Ulbp1-pGL3 luciferase reporter plasmids, 10 ng of pRL-CMV plasmid (Promega) encoding Renilla luciferase, and 140 ng of mouse CHOP expression plasmid (pcDNA3.1[−]-mDdit3 or pcDNA3.1[−]) using Lipofectamine 2000 reagent (Invitrogen), as recommended by the manufacturer's instruction. The reporter gene activities were measured by a dual-luciferase reporter assay system (Promega), according to the manufacturer's instructions (Promega), 24 h after transfection. Data were normalized against Renilla luciferase activity.

Cytotoxic assay

Primary mouse NK cells were isolated from mouse spleens using NK cell isolation kits (Miltenyi Biotec) according to the manufacturer's instruction. The NK cells were cultured in RPMI-1640 medium supplemented with 10% FBS and 200 U/ml recombinant human IL-2 for one week. IELs were isolated as described in the Reporter assay section. In some experiments, the effector cells were pretreated with anti-NKG2D (clone CX5)–blocking antibodies or an isotype-matched control Ig for 30 min at 4°C. Target cells were labeled with 2 mM CFSE (Molecular Probes) for 10 min at 37°C. After incubation with effector cells for 4 h at 37°C at the indicated effector/target (E:T) ratio, cells were stained with 7-aminoactinomycin D (7-AAD; BioLegend) for 15 min and analyzed by flow cytometry. The specific cytotoxicity was calculated as (number of double-positive cells for CFSE and 7-AAD)/(CFSE positive cells) × 100%.

Anti-NKG2D in vivo treatment and group 1 ILC depletion experiments

$Xbp1^{T\text{-}\Delta IEC}$ mice were treated with anti-NKG2D blockade antibody (CX5) or an isotype-matched control Ig (200 µg/injection) intraperitoneally on days −1 and 2 after tamoxifen injection, and small intestines were collected on day 7 after tamoxifen injection. Similarly, $Xbp1^{T\text{-}\Delta IEC}$ mice were treated with 200 µg anti-NK1.1 antibody (PK136) or isotype-matched Ig control, with anti-asialo–GM1 (10 µl per mouse) on day −1 of tamoxifen injection, to ensure efficient depletion of $NK1.1^+$ cells in the intraepithelial compartment of the intestine. $NK1.1^+$ cell depletion was confirmed on day 7 after administration of tamoxifen using flow cytometry.

Statistical analysis

Statistical significance was calculated using an unpaired two-tailed Student's *t* test or a Mann–Whitney *U* test, when appropriate, and considered significant at $P < 0.05$. In experiments comparing more than two groups, one-way ANOVA with Bonferroni's posthoc testing was performed. Data were analyzed using GraphPad Prism software (GraphPad Software, Inc.).

Online supplemental material

Fig. S1 A shows *Xbp1* expression in shCtrl and *shXbp1* MODE-K cells. Fig. S1 B shows the stability of *Ulbp1* mRNA in shCtrl and *shXbp1* MODE-K cells. Fig. S1, C and D, reveals MHC class I expression on XBP1-deficient epithelial cells. Fig. S1, E–G, demonstrates ER stress–related factors in XBP1-deficient epithelial cells. Fig. S2 shows the gating strategy of iIELs in XBP1-deficient mice. Fig. S3 shows transcriptional analysis of TCR-$\gamma\delta^+$ T cells obtained from the intestinal epithelium of $Xbp1^{\Delta IEC}$ mice. Fig. S4 A shows immunohistochemistry for lysozyme and Alcian blue staining. Fig. S4, B and C, depicts the intranuclear EOMES expression on intraepithelial $CD3^-$ $CD19^-$ $NK1.1^+$ cells. Fig S4, D and E, shows NKG2D expression on intraepithelial $CD3^+$ $NK1.1^+$ cells. Fig. S5 shows higher cytotoxicity of iIELs from $Xbp1^{\Delta IEC}$ mice compared with iIELs from wild-type mice.

ACKNOWLEDGMENTS

This work was supported by the National Institutes of Health (grants DK044319, DK051362, DK053056, and DK088199 and grant to the Harvard Digestive Diseases Center DK034854 to R. Blumberg), Crohn's and Colitis Foundation of America (grant 3670 to M.B. Flak), Instituto de Salud Carlos III from Spain (grant PI13/00218 to E. Martinez-Naves), Netherlands Organization for Scientific Research (Rubicon grant 825.13.012 to J. Grootjans), Japan Society for the Promotion of Science (KAKENHI grants 2689323 and 16K19162 to S. Hosomi), Deutsche Forschungsgemeinschaft (grant KR 4749/1-1 to N. Krupka), and Pediatric Scientist Development Program (grant K12-HD000850 to J.D. Matute). L.L. Lanier is an American Cancer Society Professor and funded by National Institutes of Health grants AI066897 and AI068129.

L.L. Lanier and the University of California, San Francisco have licensed intellectual property rights regarding NKG2D for commercial applications. The authors declare no further competing financial interests.

Submitted: 4 December 2016
Revised: 25 May 2017
Accepted: 10 July 2017

REFERENCES

Adolph, T.E., M.F. Tomczak, L. Niederreiter, H.-J. Ko, J. Böck, E. Martinez-Naves, J.N. Glickman, M. Tschurtschenthaler, J. Hartwig, S. Hosomi, et al. 2013. Paneth cells as a site of origin for intestinal inflammation. *Nature.* 503:272–276.

Allez, M., B.E. Skolnick, M. Wisniewska-Jarosinska, R. Petryka, and R.V. Overgaard. 2016. Anti-NKG2D monoclonal antibody (NNC0142-0002) in active Crohn's disease: a randomised controlled trial. *Gut*. http ://dx.doi.org/10.1136/gutjnl-2016-311824

Baker, A.M., B. Cereser, S. Melton, A.G. Fletcher, M. Rodriguez-Justo, P.J. Tadrous, A. Humphries, G. Elia, S.A. McDonald, N.A. Wright, et al. 2014. Quantification of crypt and stem cell evolution in the normal and neoplastic human colon. *Cell Reports.* 8:940–947. http://dx.doi.org/10 .1016/j.celrep.2014.07.019

Bartolome, A., C. Guillen, and M. Benito. 2012. Autophagy plays a protective role in endoplasmic reticulum stress-mediated pancreatic β cell death. *Autophagy.* 8:1757–1768. http://dx.doi.org/10.4161/auto.21994

Bernink, J.H., L. Krabbendam, K. Germar, E. de Jong, K. Gronke, M. Kofoed-Nielsen, J.M. Munneke, M.D. Hazenberg, J. Villaudy, C.J. Buskens, et al. 2015. Interleukin-12 and -23 control plasticity of CD127^{+} group 1 and group 3 innate lymphoid cells in the intestinal lamina propria. *Immunity.* 43:146–160. http://dx.doi.org/10.1016/j.immuni.2015.06.019

Bogaert, S., M. De Vos, K. Olievier, H. Peeters, D. Elewaut, B. Lambrecht, P. Pouliot, and D. Laukens. 2011. Involvement of endoplasmic reticulum stress in inflammatory bowel disease: a different implication for colonic and ileal disease? *PLoS One.* 6:e25589. http://dx.doi.org/10.1371/journal.pone.0025589

Champsaur, M., and L.L. Lanier. 2010. Effect of NKG2D ligand expression on host immune responses. *Immunol. Rev.* 235:267–285. http://dx.doi.org/10.1111/j.0105-2896.2010.00893.x

Chen, G.E., H. Wu, J. Ma, S.J. Chadban, and A. Sharland. 2011a. Toll-like receptor 4 engagement contributes to expression of NKG2D ligands by renal tubular epithelial cells. *Nephrol. Dial. Transplant.* 26:3873–3881. http://dx.doi.org/10.1093/ndt/gfr234

Chen, Z., L. Chen, K. Baker, T. Olszak, S. Zeissig, Y.H. Huang, T.T. Kuo, O. Mandelboim, N. Beauchemin, L.L. Lanier, and R.S. Blumberg. 2011b. CEACAM1 dampens antitumor immunity by down-regulating NKG2D ligand expression on tumor cells. *J. Exp. Med.* 208:2633–2640. http://dx.doi.org/10.1084/jem.20102575

Deuring, J.J., G.M. Fuhler, S.R. Konstantinov, M.P. Peppelenbosch, E.J. Kuipers, C. de Haar, and C.J. van der Woude. 2014. Genomic ATG16L1 risk allele-restricted Paneth cell ER stress in quiescent Crohn's disease. *Gut.* 63:1081–1091. http://dx.doi.org/10.1136/gutjnl-2012-303527

Ebihara, T., H. Masuda, T. Akazawa, M. Shingai, H. Kikuta, T. Ariga, M. Matsumoto, and T. Seya. 2007. Induction of NKG2D ligands on human dendritic cells by TLR ligand stimulation and RNA virus infection. *Int. Immunol.* 19:1145–1155. http://dx.doi.org/10.1093/intimm/dxm073

El Marjou, F., K.P. Janssen, B.H. Chang, M. Li, V. Hindie, L. Chan, D. Louvard, P. Chambon, D. Metzger, and S. Robine. 2004. Tissue-specific and inducible Cre-mediated recombination in the gut epithelium. *Genesis.* 39:186–193. http://dx.doi.org/10.1002/gene.20042

Eri, R.D., R.J. Adams, T.V. Tran, H. Tong, I. Das, D.K. Roche, I. Oancea, C.W. Png, P.L. Jeffery, G.L. Radford-Smith, et al. 2011. An intestinal epithelial defect conferring ER stress results in inflammation involving both innate and adaptive immunity. *Mucosal Immunol.* 4:354–364. http://dx.doi.org/10.1038/mi.2010.74

Fuchs, A., W. Vermi, J.S. Lee, S. Lonardi, S. Gilfillan, R.D. Newberry, M. Cella, and M. Colonna. 2013. Intraepithelial type 1 innate lymphoid cells are a unique subset of IL-12- and IL-15-responsive IFN-γ-producing cells. *Immunity.* 38:769–781. http://dx.doi.org/10.1016/j.immuni.2013.02.010

Gasser, S., S. Orsulic, E.J. Brown, and D.H. Raulet. 2005. The DNA damage pathway regulates innate immune system ligands of the NKG2D receptor. *Nature.* 436:1186–1190. http://dx.doi.org/10.1038/nature03884

Gowen, B.G., B. Chim, C.D. Marceau, T.T. Greene, P. Burr, J.R. Gonzalez, C.R. Hesser, P.A. Dietzen, T. Russell, A. Iannello, et al. 2015. A forward genetic screen reveals novel independent regulators of ULBP1, an activating ligand for natural killer cells. *eLife.* 4:e08474. http://dx.doi.org/10.7554/eLife.08474

Groh, V., S. Bahram, S. Bauer, A. Herman, M. Beauchamp, and T. Spies. 1996. Cell stress-regulated human major histocompatibility complex class I gene expressed in gastrointestinal epithelium. *Proc. Natl. Acad. Sci. USA.* 93:12445–12450. http://dx.doi.org/10.1073/pnas.93.22.12445

Grootjans, J., A. Kaser, R.J. Kaufman, and R.S. Blumberg. 2016. The unfolded protein response in immunity and inflammation. *Nat. Rev. Immunol.* 16:469–484. http://dx.doi.org/10.1038/nri.2016.62

Haas, J.D., F.H. González, S. Schmitz, V. Chennupati, L. Föhse, E. Kremmer, R. Förster, and I. Prinz. 2009. CCR6 and NK1.1 distinguish between IL-17A and IFN-γ-producing γδ effector T cells. *Eur. J. Immunol.* 39:3488–3497. http://dx.doi.org/10.1002/eji.200939922

Hamerman, J.A., K. Ogasawara, and L.L. Lanier. 2004. Cutting edge: Toll-like receptor signaling in macrophages induces ligands for the NKG2D receptor. *J. Immunol.* 172:2001–2005. http://dx.doi.org/10.4049/jimmunol.172.4.2001

Heazlewood, C.K., M.C. Cook, R. Eri, G.R. Price, S.B. Tauro, D. Taupin, D.J. Thornton, C.W. Png, T.L. Crockford, R.J. Cornall, et al. 2008. Aberrant mucin assembly in mice causes endoplasmic reticulum stress and spontaneous inflammation resembling ulcerative colitis. *PLoS Med.* 5:e54. http://dx.doi.org/10.1371/journal.pmed.0050054

Himmelreich, H., A. Mathys, A. Wodnar-Filipowicz, and C.P. Kalberer. 2011. Post-transcriptional regulation of ULBP1 ligand for the activating immunoreceptor NKG2D involves 3′ untranslated region. *Hum. Immunol.* 72:470–478. http://dx.doi.org/10.1016/j.humimm.2011.03.005

Hüe, S., J.J. Mention, R.C. Monteiro, S. Zhang, C. Cellier, J. Schmitz, V. Verkarre, N. Fodil, S. Bahram, N. Cerf-Bensussan, and S. Caillat-Zucman. 2004. A direct role for NKG2D/MICA interaction in villous atrophy during celiac disease. *Immunity.* 21:367–377. http://dx.doi.org/10.1016/j.immuni.2004.06.018

Iwakoshi, N.N., A.-H. Lee, P. Vallabhajosyula, K.L. Otipoby, K. Rajewsky, and L.H. Glimcher. 2003. Plasma cell differentiation and the unfolded protein response intersect at the transcription factor XBP-1. *Nat. Immunol.* 4:321–329. http://dx.doi.org/10.1038/ni907

Jia, W., H.H. Pua, Q.J. Li, and Y.W. He. 2011. Autophagy regulates endoplasmic reticulum homeostasis and calcium mobilization in T lymphocytes. *J. Immunol.* 186:1564–1574. http://dx.doi.org/10.4049/jimmunol.1001822

Kaser, A., A.H. Lee, A. Franke, J.N. Glickman, S. Zeissig, H. Tilg, E.E.S. Nieuwenhuis, D.E. Higgins, S. Schreiber, L.H. Glimcher, and R.S. Blumberg. 2008. XBP1 links ER stress to intestinal inflammation and confers genetic risk for human inflammatory bowel disease. *Cell.* 134:743–756. http://dx.doi.org/10.1016/j.cell.2008.07.021

Kaser, A., M.B. Flak, M.F. Tomczak, and R.S. Blumberg. 2011. The unfolded protein response and its role in intestinal homeostasis and inflammation. *Exp. Cell Res.* 317:2772–2779. http://dx.doi.org/10.1016/j.yexcr.2011.07.008

Keilbaugh, S.A., M.E. Shin, R.F. Banchereau, L.D. McVay, N. Boyko, D. Artis, J.J. Cebra, and G.D. Wu. 2005. Activation of RegIIIβ/γ and interferon γ expression in the intestinal tract of SCID mice: an innate response to bacterial colonisation of the gut. *Gut.* 54:623–629. http://dx.doi.org/10.1136/gut.2004.056028

Kim, I., W. Xu, and J.C. Reed. 2008. Cell death and endoplasmic reticulum stress: disease relevance and therapeutic opportunities. *Nat. Rev. Drug Discov.* 7:1013–1030. http://dx.doi.org/10.1038/nrd2755

Lanier, L.L. 2015. NKG2D receptor and its ligands in host defense. *Cancer Immunol. Res.* 3:575–582. http://dx.doi.org/10.1158/2326-6066.CIR-15-0098

León, F., E. Roldán, L. Sanchez, C. Camarero, A. Bootello, and G. Roy. 2003. Human small-intestinal epithelium contains functional natural killer lymphocytes. *Gastroenterology.* 125:345–356. http://dx.doi.org/10.1016/S0016-5085(03)00886-2

Lu, M., D.A. Lawrence, S. Marsters, D. Acosta-Alvear, P. Kimmig, A.S. Mendez, A.W. Paton, J.C. Paton, P. Walter, and A. Ashkenazi. 2014. Opposing unfolded-protein-response signals converge on death receptor 5 to control apoptosis. *Science.* 345:98–101. http://dx.doi.org/10.1126/science.1254312

Olszak, T., J.F. Neves, C.M. Dowds, K. Baker, J. Glickman, N.O. Davidson, C.S. Lin, C. Jobin, S. Brand, K. Sotlar, et al. 2014. Protective mucosal immunity mediated by epithelial CD1d and IL-10. *Nature.* 509:497–502. http://dx.doi.org/10.1038/nature13150

Ono, Y., F. Hirai, T. Matsui, T. Beppu, Y. Yano, N. Takatsu, Y. Takaki, T. Nagahama, T. Hisabe, K. Yao, et al. 2012. Value of concomitant endoscopic balloon dilation for intestinal stricture during long-term infliximab therapy in

patients with Crohn's disease. *Dig. Endosc.* 24:432–438. http://dx.doi.org/10.1111/j.1443-1661.2012.01315.x

Ouellette, A.J. 2010. Paneth cells and innate mucosal immunity. *Curr. Opin. Gastroenterol.* 26:547–553. http://dx.doi.org/10.1097/MOG.0b013e32833dccde

Peterson, L.W., and D. Artis. 2014. Intestinal epithelial cells: regulators of barrier function and immune homeostasis. *Nat. Rev. Immunol.* 14:141–153. http://dx.doi.org/10.1038/nri3608

Rabinovich, B.A., J. Li, J. Shannon, R. Hurren, J. Chalupny, D. Cosman, and R.G. Miller. 2003. Activated, but not resting, T cells can be recognized and killed by syngeneic NK cells. *J. Immunol.* 170:3572–3576. http://dx.doi.org/10.4049/jimmunol.170.7.3572

Raulet, D.H. 2003. Roles of the NKG2D immunoreceptor and its ligands. *Nat. Rev. Immunol.* 3:781–790. http://dx.doi.org/10.1038/nri1199

Raulet, D.H., and N. Guerra. 2009. Oncogenic stress sensed by the immune system: role of natural killer cell receptors. *Nat. Rev. Immunol.* 9:568–580. http://dx.doi.org/10.1038/nri2604

Rhodes, K.A., E.M. Andrew, D.J. Newton, D. Tramonti, and S.R. Carding. 2008. A subset of IL-10-producing γδ T cells protect the liver from *Listeria*-elicited, $CD8^+$ T cell-mediated injury. *Eur. J. Immunol.* 38:2274–2283. http://dx.doi.org/10.1002/eji.200838354

Robinette, M.L., A. Fuchs, V.S. Cortez, J.S. Lee, Y. Wang, S.K. Durum, S. Gilfillan, M. Colonna, L. Shaw, B. Yu, et al. Immunological Genome Consortium. 2015. Transcriptional programs define molecular characteristics of innate lymphoid cell classes and subsets. *Nat. Immunol.* 16:306–317. http://dx.doi.org/10.1038/ni.3094

Salzman, N.H., K. Hung, D. Haribhai, H. Chu, J. Karlsson-Sjöberg, E. Amir, P. Teggatz, M. Barman, M. Hayward, D. Eastwood, et al. 2010. Enteric defensins are essential regulators of intestinal microbial ecology. *Nat. Immunol.* 11:76–82. http://dx.doi.org/10.1038/ni.1825

Shiohara, T., N. Moriya, J. Hayakawa, S. Itohara, and H. Ishikawa. 1996. Resistance to cutaneous graft-vs.-host disease is not induced in T cell receptor delta gene-mutant mice. *J. Exp. Med.* 183:1483–1489. http://dx.doi.org/10.1084/jem.183.4.1483

Sips, M., G. Sciaranghella, T. Diefenbach, A.S. Dugast, C.T. Berger, Q. Liu, D. Kwon, M. Ghebremichael, J.D. Estes, M. Carrington, et al. 2012. Altered distribution of mucosal NK cells during HIV infection. *Mucosal Immunol.* 5:30–40. http://dx.doi.org/10.1038/mi.2011.40

Smith, P.D., T.T. MacDonald, and R.S. Blumberg. Society for Mucosal Immunology. 2013. Principles of mucosal immunology. Taylor & Francis Group, London. 529 pp.

Spits, H., J.H. Bernink, and L. Lanier. 2016. NK cells and type 1 innate lymphoid cells: partners in host defense. *Nat. Immunol.* 17:758–764. http://dx.doi.org/10.1038/ni.3482

Stern-Ginossar, N., C. Gur, M. Biton, E. Horwitz, M. Elboim, N. Stanietsky, M. Mandelboim, and O. Mandelboim. 2008. Human microRNAs regulate stress-induced immune responses mediated by the receptor NKG2D. *Nat. Immunol.* 9:1065–1073. http://dx.doi.org/10.1038/ni.1642

Tagliabue, A., A.D. Befus, D.A. Clark, and J. Bienenstock. 1982. Characteristics of natural killer cells in the murine intestinal epithelium and lamina propria. *J. Exp. Med.* 155:1785–1796. http://dx.doi.org/10.1084/jem.155.6.1785

Todd, D.J., A.-H. Lee, and L.H. Glimcher. 2008. The endoplasmic reticulum stress response in immunity and autoimmunity. *Nat. Rev. Immunol.* 8:663–674. http://dx.doi.org/10.1038/nri2359

Ubeda, M., X.Z. Wang, H. Zinszner, I. Wu, J.F. Habener, and D. Ron. 1996. Stress-induced binding of the transcriptional factor CHOP to a novel DNA control element. *Mol. Cell. Biol.* 16:1479–1489. http://dx.doi.org/10.1128/MCB.16.4.1479

Venkataraman, G.M., D. Suciu, V. Groh, J.M. Boss, and T. Spies. 2007. Promoter region architecture and transcriptional regulation of the genes for the MHC class I-related chain A and B ligands of NKG2D. *J. Immunol.* 178:961–969. http://dx.doi.org/10.4049/jimmunol.178.2.961

Vidal, K., I. Grosjean, J.P. evillard, C. Gespach, and D. Kaiserlian. 1993. Immortalization of mouse intestinal epithelial cells by the SV40-large T gene: Phenotypic and immune characterization of the MODE-K cell line. *J. Immunol. Methods.* 166:63–73. http://dx.doi.org/10.1016/0022-1759(93)90329-6

Wang, X., and B. Seed. 2003. A PCR primer bank for quantitative gene expression analysis. *Nucleic Acids Res.* 31:e154. http://dx.doi.org/10.1093/nar/gng154

Wencker, M., G. Turchinovich, R. Di Marco Barros, L. Deban, A. Jandke, A. Cope, and A.C. Hayday. 2014. Innate-like T cells straddle innate and adaptive immunity by altering antigen-receptor responsiveness. *Nat. Immunol.* 15:80–87. http://dx.doi.org/10.1038/ni.2773

Zeissig, S., A. Kaser, S.K. Dougan, E.E. Nieuwenhuis, and R.S. Blumberg. 2007. Role of NKT cells in the digestive system. III. Role of NKT cells in intestinal immunity. *Am. J. Physiol. Gastrointest. Liver Physiol.* 293:G1101–G1105. http://dx.doi.org/10.1152/ajpgi.00342.2007